JOURNAL OF MATERIALS SCIENCE 30 (1995) 4720–4725

Numerical study of the specimen size effect in the split Hopkinson pressure bar tests

J. RODRÍGUEZ, R. CORTÉS, M. A. MARTÍNEZ, V. SÁNCHEZ-GÁLVEZ
Department of Materials Science, E.T.S.I de Caminos, Canales y Puertos, Polytechnic University of Madrid, Ciudad Universitaria s/n, 28040 Madrid, Spain

C. NAVARRO
Department of Engineering, Carlos III University, Butarque 15, 28911 Leganés, Madrid, Spain

A numerical and experimental assessment of the compression test in the split Hopkinson pressure bar (SHPB) has been made. The DYNA2D finite element code was employed in the numerical part. The aim of the work was to establish the influence of an important reduction in the specimen diameter on the results. To this end, several numerical experiments were carried out with different diameters. Experimental measurements using the SHPB technique were also performed. The material studied was the 7017 T73 aluminium alloy. In the simulations, stress histories were registered at different places in the incident and output bars, as well as in the test specimen. Numerical simulations show important three-dimensional effects in the SHPB, increasing for smaller diameters. Experiments show the same tendencies evinced by the numerical simulation. Care must be taken to minimize them to achieve the desirable uniaxial stress condition on the specimen.

1. Introduction

Since the development of the Kolsky apparatus (also called the split Hopkinson pressure bar, SHPB) several decades ago [1], such a device has become widely used for testing the behaviour of materials at high rates of strain. As is well-known, in this testing procedure, a cylindrical specimen is placed between two long elastic bars. At the free end of the first one, called the incident bar, a stress pulse is applied by either an explosive or the impact of a projectile. The generated compression pulse propagates along the incident bar, and a part of it is reflected at the bar/specimen interface, whereas the residual part is transmitted through the specimen to the second bar (called the output bar). Because both bars behave elastically, measurements of strains or displacements in the bars may provide the dynamic stress–strain curve of the specimen material [1,2]. The basic assumptions of the test are (a) the bars/specimen system is in a uni-dimensional stress state, and (b) the strain distribution in the specimen is homogeneous. Results of the application of this method to estimate the dynamic properties of metallic materials are found in the open literature [3–6].

In the past, efforts have been devoted to estimate the influence of factors such as friction or inertia on test results [7–9]. It is recognized that the friction effects decrease as the length/diameter ratio increases. On the other hand, inertial effects have a more complicated dependence on test parameters. Davies and Hunter [7] used an appealing experimental measuring technique, where contributions of axial and radial inertia have opposite signs, and concluded that for a slenderness ratio (or length to diameter ratio) equal to $\sqrt{3/4}$ (for an incompressible material), both terms annihilate and inertia effects may be ignored. However, when the strain rate is not constant during the test, the inertia effects may increase substantially for larger values of the slenderness ratio. Thus, a compromise value for the length–diameter ratio is required, which in a first trial may be around 0.5 [8]. The influence of the shape of the stress pulse on test results has also been demonstrated, and a trapezoidal shape has been found to be more appropriate than a triangular one [10,11]. Jashman [10] found that although for both types of pulse the elastic modulus was lower than the reference one, the plastic modulus was better approximated by the trapezoidal pulse. Similar results were found by Buchar *et al.* [11]. In some simulated experiments, these authors also found that an increase in specimen length may give a better approximation to the actual mechanical behaviour of the material [11]. This result disagrees with previous results obtained by Bertholf and Karnes [8], but the discrepancy may be associated with different simulation conditions in the numerical analysis. Recently, the importance of the dispersion effects has also been shown, and attempts to overcome this problem have been made [12,13]. Such dispersion corrections are based on analytical solutions of longitudinal wave propagation in an infinitely long cylinder obtained by a Pochhammer–Chree analysis, and by assuming that a particular vibration mode predominates during the test. However, this solution may not be exact for finite cylinders (in which case will be actually applied), because it does

0022–2461

not fulfil the boundary conditions at the end of the bars.

In this work, the compression test in the split Hopkinson pressure bar was numerically and experimentally studied. The DYNA2D commercial lagrangian code for dynamic problems was used in the numerical part [14]. With this tool, experiments performed with several specimen sizes are numerically simulated. Detailed time histories of stresses and displacements at different places are recorded. Then the estimated stress-strain behaviour of the specimen is compared to that previously assumed and the influence of specimen geometry is investigated. This work tries to estimate the effect of an important reduction in the specimen diameter (bar diameter held constant), because some researchers reduce the specimen diameter to reach higher and more constant strain rates. Experimental tests performed in 7017 T73 aluminium alloy show the same tendencies envisaged in the numerical simulations. It is concluded that a one-dimensional stress-state is very difficult to achieve in practice and the three-dimensional effects are increased when the specimen diameter relative to the bar diameter is reduced. Furthermore, the specimen diameter cannot be reduced beyond a certain limit, below which a departure from the actual material response is evident.

2. Experimental procedure

Dynamic compression tests were made in the SHPB, for a 7017 T73 aluminium alloy. This alloy was selected because its mechanical behaviour has been found to be nearly independent upon the strain rate, which simplifies the comparison between analysis and experiment. Chemical composition of this alloy is 5.1% Zn, 2.4% Mg, 0.3% Fe, 0.16% Si, 0.12% Cu, 0.22% Mn, 0.16% Cr, 0.12% Zr, Al balance. This material has a Young's modulus of 71 GPa. Furthermore, its simple tension test properties in static conditions are an elastic limit of 450 MPa, a tensile strength of 499 MPa, and a rupture strain of 12% in 50 mm.

Experiments with 21.6, 14, 10 and 7 mm diameter specimens with a slenderness ratio $l/d = 0.5$, were performed. Contact interfaces were lubricated with S_2Mo, giving very good lubrication properties. The impact velocity of the projectile was about 15–16 $m\,s^{-1}$, giving rise to a compression wave with a peak value near 300 MPa.

In the experiments, the strain histories in the bars corresponding to the incident, ε_i, reflected, ε_r, and transmitted wave, ε_t (see Fig. 1), were determined. The stresses, σ, and velocities, v, were estimated at the end of the bars, from the well-known expressions for the split Hopkinson pressure bar theory

$$\sigma_{inp} = E(\varepsilon_i + \varepsilon_r) \quad (1)$$

$$\sigma_{out} = E\varepsilon_t \quad (2)$$

$$v_{inp} = -c(\varepsilon_i - \varepsilon_r) \quad (3)$$

$$v_{out} = -c\varepsilon_t \quad (4)$$

where E is Young's modulus of the bars and c is the propagation velocity of the compression waves. The

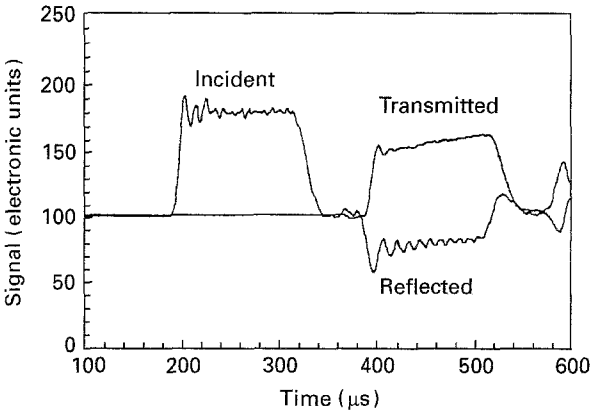

Figure 1 Experimental values of the incident, reflected and transmitted waves.

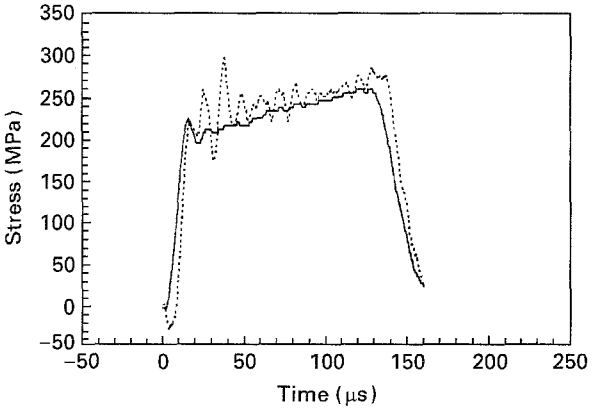

Figure 2 Experimental values of the (– – –) input and (——) output bar stresses.

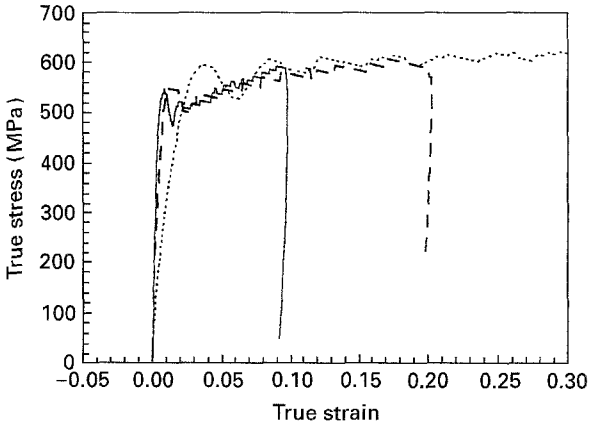

Figure 3 Experimental stress–strain curves for different diameters: (——) 14 mm, (– – –) 10 mm, (---) 7 mm.

subscripts refer to the input (inp) and output (out) bars, respectively. Finally, stress, σ, strain rate, $\dot{\varepsilon}$, and strain, ε, in the specimen are computed as

$$\sigma = \frac{A_b}{2A_s}(\sigma_{inp} + \sigma_{out}) = \frac{EA_b}{2A_s}(\varepsilon_i + \varepsilon_r + \varepsilon_t) \quad (5)$$

$$\dot{\varepsilon} = \frac{v_{out} - v_{inp}}{l} = -\frac{c}{l}(\varepsilon_t + \varepsilon_r - \varepsilon_i) \quad (6)$$

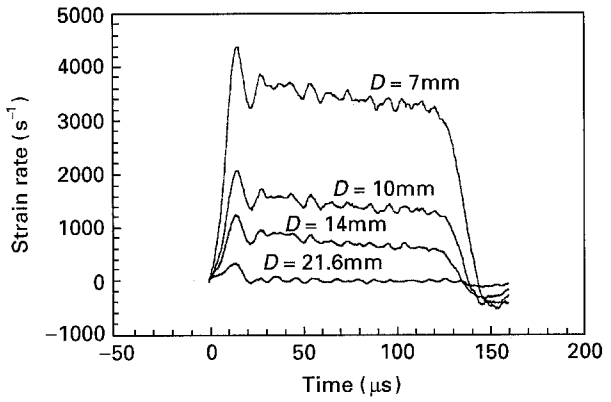

Figure 4 Experimental strain rate–strain curves for different diameters.

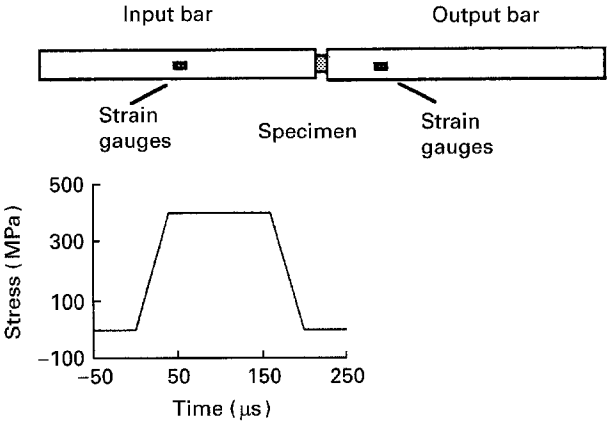

Figure 6 Schematic illustrations of the bars system and stress pulse.

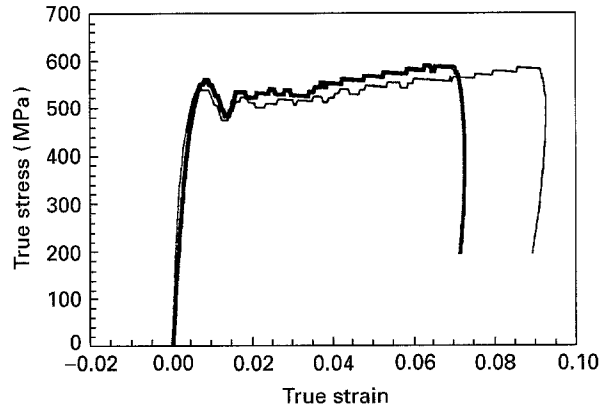

Figure 5 Effect of lubrication in the experimental stress–strain curves. (——) unlubricated, (——) lubricated.

and

$$\varepsilon = \int_0^t \dot{\varepsilon}\, dt \tag{7}$$

where l is the specimen length, and A_b and A_s are the cross-sectional areas of bars and specimen, respectively. Equations 5–7 correspond to the traditional procedure. Nevertheless, this work supports the tendency to use only the output bar stress to calculate the stress in the specimen. This is reasonable because the input bar stress is affected by a higher number of spureous oscillations. The histories of both stresses versus time are plotted in Fig. 2, where the problem is clearly shown. Therefore, rather than employing Equation 5, the stress in the specimen computed as

$$\sigma = \frac{A_b}{A_s} E \varepsilon_t \tag{8}$$

Fig. 3 depicts the true stress–strain curves determined from the experiments for the different diameters selected. For a specimen diameter of 21.6 mm, material remained in the elastic regime. It is clearly seen in such a figure that the diameter is reduced to 7 mm, although a larger plastic strain is reached, larger inaccuracies in the stress–strain curve are observed. Moreover, elastic strains are overestimated for the smaller diameters. Fig. 4 shows the strain–rate histories in the tested specimens for the different diameters. It is obvious that the strain rate during the tests increases as the specimen diameter decreases. Fig. 5 allows comparison of the true stress–strain curves obtained with and without lubrication.

3. Description of the numerical analysis

The DYNA2D finite element code was employed to analyse the dynamic response of two bars of 1.0 m length and 22.0 mm diameter, modelled by means of 2107 nodes and 1800 quadrilateral elements (300 along the axial direction and 6 along the radius). Between the bars, specimens with a constant length/diameter ratio of 0.5 are modelled using 169 nodes and 144 quadrilateral elements (12 along the axial direction and 12 along the radius). The specimen diameters analysed are 14, 10 and 7 mm. The whole problem involves 4383 nodes and 3744 elements. Owing to the axial symmetry of the system, it is necessary to model only one-half of the diametral plane of the specimen/bars system. The behaviour of the specimen material corresponds to that of the 7017 T73 aluminium alloy. It is assumed to be bilinear elastic–plastic and strain-rate independent. Values used are a Young's modulus of 71 GPa, a yield stress of 500 MPa, a stress–strain slope in the plastic region of 0.62 GPa and a density of 2700 kg m^{-3}. The material of the bars was assumed fully elastic, with a Young's modulus of 202 GPa and a density of 7850 kg m^{-3}, typical values of steel. A trapezoidal stress pulse was applied at the end of the incident bar. Its total duration was 200 μs, with a rise time and a descent time both equal to 20 μs. The peak stress value was 400 MPa. Schematic illustrations of the bars/specimen system and stress pulse are illustrated in Fig. 6.

Spurious numerical oscillations are always present in modelling stress-wave propagation. To circumvent this problem, the code uses an artificial dissipative term added to the pressure and composed of a linear and a quadratic term in the velocity gradient components [15,16]. In this manner, with a suitable choice of the pertinent coefficients, artificial numerical oscillations are damped out, whereas the physical components of the solution remain unaffected. The introduction of damping, through artificial viscosity, may produce some distortion of the solution, but

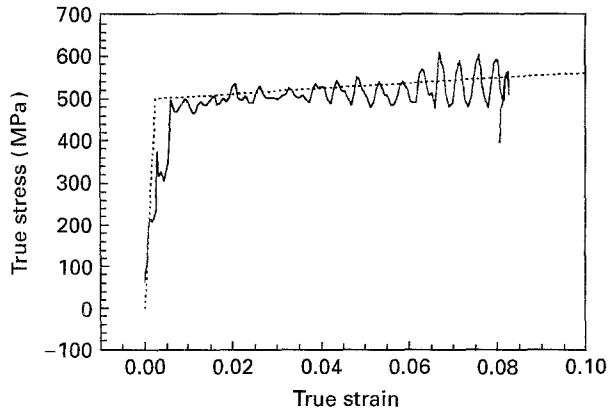

Figure 7 Numerical true stress–true strain curve for 14 mm diameter: (– – –) assumed, (——) obtained.

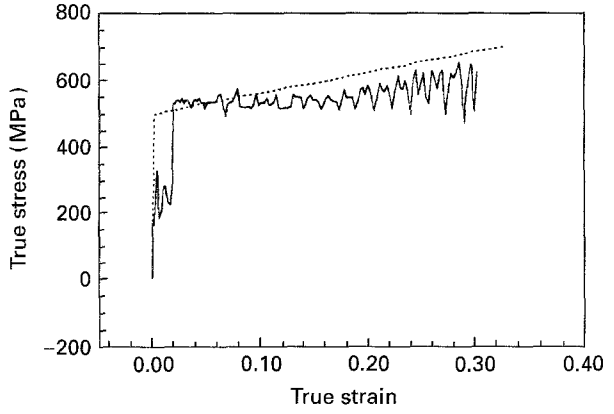

Figure 8 Numerical true stress–true strain curve for 10 mm diameter: (– – –) assumed, (——) obtained.

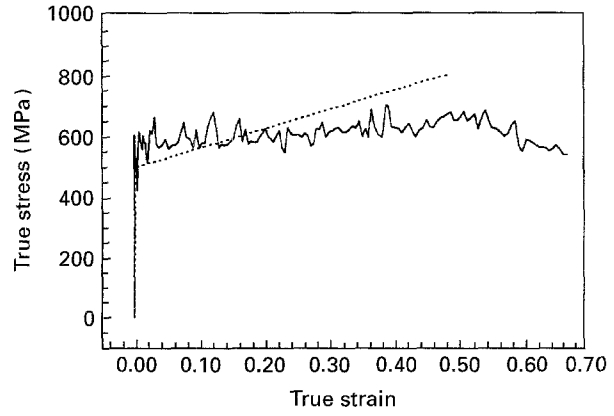

Figure 9 Numerical true stress–true strain curve for 7 mm diameter: (– – –) assumed, (——) obtained.

this effect is reduced to a minimum with an adequate selection of the viscosity parameters, according to well-established criteria. In our case, a linear-term coefficient of 0.3 and a quadratic-term coefficient of 2.0 were used. To check the appropriateness of the values chosen, records of stress versus time in various positions of the bar were compared. Little differences between these pulses can be observed, showing that the artificial viscosity terms do not affect the main (physical) terms of the solution.

4. Numerical results

In Figs 7–9 the true stress–true strain curves obtained from the numerical computations, by using the same equations as in the experiments, are shown for different bar diameters. Such curves are also compared with the bilinear stress–strain curve assumed for the specimen material in the numerical analysis. The curves obtained from the calculations for the 14 and 10 mm diameters, provide a relatively good approximation to the assumed material behaviour in all cases, although for the smallest diameters, the curves exhibit a number of oscillations of a relatively high amplitude. In all cases, the approximation is good whenever the plastic strain exceeds a value of about 0.01. As the specimen diameter decreases, the amplitude of the oscillations increases, thus resulting in some uncertainties in the estimation of the stress–strain curve. This is particularly true for the 7 mm diameter specimen, where the amplitude of the oscillations is excessive to obtain a reliable estimation of the stress–strain curve. Moreover, smaller stress values for the plastic range than the assumed behaviour are evident from Fig. 9. It is also derived from the calculations that the material hardening is masked using this diameter.

Common to all the specimen diameters analysed is the overestimation in the elastic strain; consequently, the elastic modulus computed is much lower than the reference one. Obviously, total deformation is higher when the specimen diameter is reduced.

The strain rate is not constant during the whole test. This is very common in compression tests because there are two factors reducing the strain rate, namely, material hardening and the increase in the specimen cross-sectional area during the deformation process. However, it is clear from Fig. 4 that the strain rate is much higher for the smaller diameters.

Another important difference can be derived from the results of specimens of different sizes, namely, an increase in the initial time interval where the strain rate increases very fast, from zero to the peak value. This region is wider as the specimen diameter increases. In these cases the maximum strain rate is reached later, that is, for higher plastic strain values. In all the cases studied, it is not possible to give a definite value for the strain rate. These results are also confirmed if the material conditions used in the numerical model are changed. A second numerical analysis has been carried out with the following material properties: bilinear elastic–plastic and strain-rate independent material with a Young's modulus of 71 GPa, a yield stress of 300 MPa, a stress–strain slope in the plastic region of 2 GPa and a density of 2700 $kg\,m^{-3}$. The same tendencies were observed.

5. Discussion and conclusion

Although the stress–strain relationship obtained with the SHPB is, in general, in good agreement with the

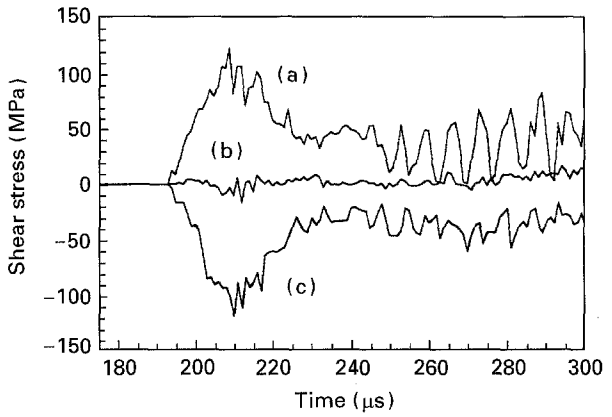

Figure 10 Numerical shear stress histories at the axis of symmetry of the specimen ($D = 7$ mm): (a) close to the input bar, (b) middle of the specimen, (c) close to the output bar.

actual behaviour of the material at high rates of strain, it is essential to take into account the limitations associated with this type of test, as the present work has made evident.

First of all, the strain is overestimated in the elastic region. This may be a consequence of the influence of the bar stiffness in the calculations. In the actual experiments this effect is enhanced by problems associated with the surface bars/specimen contact. Thus, a reliable measurement of the elastic modulus can be hardly made by means of this technique, unless the strain be directly measured in the specimen, either by optic systems or by sticking strain gauges on the specimen surface. However, this strain overestimation has very little influence in the plastic region, where total strain values are much higher.

As mentioned in Section 1, the main objective of this work was to evaluate the effects on the test results of an important reduction in the specimen diameter, while the bar diameter is kept constant, and also to ascertain whether this reduction is acceptable as a method for achieving higher strain rates. Conclusions, according to both modelling and experiment, are positive in the sense that smaller diameters can also be used in good agreement with actual material behaviour, but several aspects are important. First, the number of oscillations in the stress–strain curve increases considerably when the specimen diameter is reduced, probably due to an increase in the triaxiality of the stress state in the bars for smaller diameters. Part of the bar end is free, and thus is in zero-stress condition. Therefore, differences between the bar axis and its lateral surface, near the end, will be higher if the specimen diameter is reduced. To illustrate this, Fig. 10 shows results from the 7 mm diameter specimen. The shear stress histories obtained from the numerical analysis at the axis of symmetry of the specimen, at points in contact with the input bar, in the middle of the specimen and in contact with the output bar, are plotted. It is appreciated that peak shear stress values of 120 MPa (about 24% of the yield stress) are reached in both cases. Thus, deviations from the assumed one-dimensional theory should not be surprising (these shear stresses do not appear in the other diameters). Moreover, the non-uniformity in the bar's stress will increase the number and also the magnitude of the oscillations in the recorded signal. Second, the strain rate is higher for smaller diameters, because more energy is available to deform the material, and it is also more constant, an advantage because the aim is to obtain the mechanical properties of the material at a definite value of the strain rate. If this quantity is variable during the test, it is not possible to define an approximate strain rate for the stress–strain curve obtained. This could lead to the conclusion that it is convenient to reduce the specimen diameter. However, it is instructive to analyse the variation of the strain rate with the strain. During the initial region of deformation, strain rate changes very rapidly up to its maximum value, and then decreases more slowly. For strains lower than that of the maximum strain rate, the results cannot be used, owing to the rapid change in the strain rate. If the initial region is compared for different specimen diameters, it can be concluded that it increases when the specimen diameter is reduced. Therefore, small specimens give higher strains and strain rates, but the unreliable initial region is enlarged.

One of the basic assumptions in this test is the equilibrium condition, which means that forces at both ends of the input and output bars must be equal. The first one is calculated through the addition of incident and reflected strain pulses. Abnormal oscillations can arise from inadequate adjustment of these two pulses, without a true relation with the material behaviour. Although the agreement between both forces is enough to ensure the equilibrium condition, it is advisable to use the output bar for determining the stress in the specimen, overcoming the irregularities.

As a final conclusion, and unless the material is very soft, and almost without strain hardening, specimens with diameters appreciably smaller than those of the bars are recommended, provided that a lower bound is not exceeded (each researcher should calibrate his own test). This is because the specimens similar in size to the bars do not provide constant strain rate during the test, and the improvement in the elastic region is insufficient compensation.

References

1. H. KOLSKY, *Proc. Phys. Soc. Ser. B* **62** (1949) 676.
2. R. J. WASLEY, "Stress Wave Propagation in Solids" (Marcel Dekker, New York, 1973).
3. U. S. LINDHOLM, *J. Mech. Phys. Solids* **12** (1964) 317.
4. F. E. HAUSER, *Exp. Mech.* **6** (1966) 395.
5. C. J. MAIDEN and S. J. GREEN, *J. Appl. Mech.* **33** (1966) 496.
6. A. J. HOLZER, *J. Eng. Mater. Technol.* **101** (1979) 231.
7. E. D. H. DAVIES and S. C. HUNTER, *J. Mech. Phys. Solids* **11** (1962) 155.
8. L. D. BERTHOLF and C. H. KARNES, *ibid.* **23** (1975) 1.
9. J. Z. MALINOWSKY and J. R. KLEPACZKO, *Int. J. Mech. Sci.* **28** (1986) 381.

10. W. E. JASHMAN, *J. Appl. Mech.* **38** (1971) 75.
11. J. BUCHAR, Z. BÍLEK and F. DUSEK, "Mechanical Behaviour of Metals at Extremely High Strain Rates", (Trans Tech Publications, Switzerland, 1986).
12. P. S. FOLLANSBEE and C. FRANTZ, *J. Eng. Mater. Technol.* **105** (1983) 61.
13. J. G. GONG, L. E. MALVEN and D. A. JENKINS, *ibid.* **112** (1990) 309.
14. J. O. HALLQUIST, "Users Manual for DYNA2D–An Explicit Two Dimensional Hydrodynamic Finite Element Code with Interactive Rezoning and Graphical Display", Report UCID-18756, Rev. 3, Lawrence Livermore National Laboratory, February 1987.
15. J. A. ZUKAS, T. NICHOLAS, H. SWIFT, L. GRESZCZUK and D. CURRAN, "Impact Dynamics", (Wiley, 1982).
16. R. LANDSHOFF, "A Numerical Method for Creating Fluid Flow in the Presence of Shocks", Los Alamos Scientific Laboratory, Rep. LA-1930 (1955).

Received 30 June 1994
and accepted 5 April 1995